

Supplementary Information

Poly(vinyl alcohol)-assisted synthesis of 3D Bi_2S_3 submicrometric structures toward feasible chip photodetector applications

Krystian Mistewicz¹, Marcin Godzierz^{2,*}, Anna Gawron², Łukasz Otulakowski², Anna Hercog^{2,3}, Klaudia Kurtyka², Sugato Hajra⁴, Hoe Joon Kim⁴

¹ Silesian University of Technology, Institute of Physics – Center for Science and Education, Krasińskiego 8 Str., 40-019 Katowice, Poland; krystian.mistewicz@polsl.pl

² Centre of Polymer and Carbon Materials, Polish Academy of Sciences, Curie-Skłodowskiej 34 Str., 41-819 Zabrze, Poland; mgodzierz@cmpw-pan.pl, agawron@cmpw-pan.pl, lotulakowski@cmpw-pan.pl, ahercog@cmpw-pan.pl, kkurtyka@cmpw-pan.pl

³ SPIN-Lab Centre for Microscopic Research on Matter, University of Silesia in Katowice, 75 Pułku Piechoty 1 str., 41-500 Chorzów, Poland; anna.hercog@us.edu.pl

⁴ Department of Robotics and Mechatronics Engineering, Daegu Gyeongbuk Institute of Science and Technology, Daegu 42988, Republic of Korea; sugatohajra@dgist.ac.kr, joonkim@dgist.ac.kr

* corresponding author: mgodzierz@cmpw-pan.pl

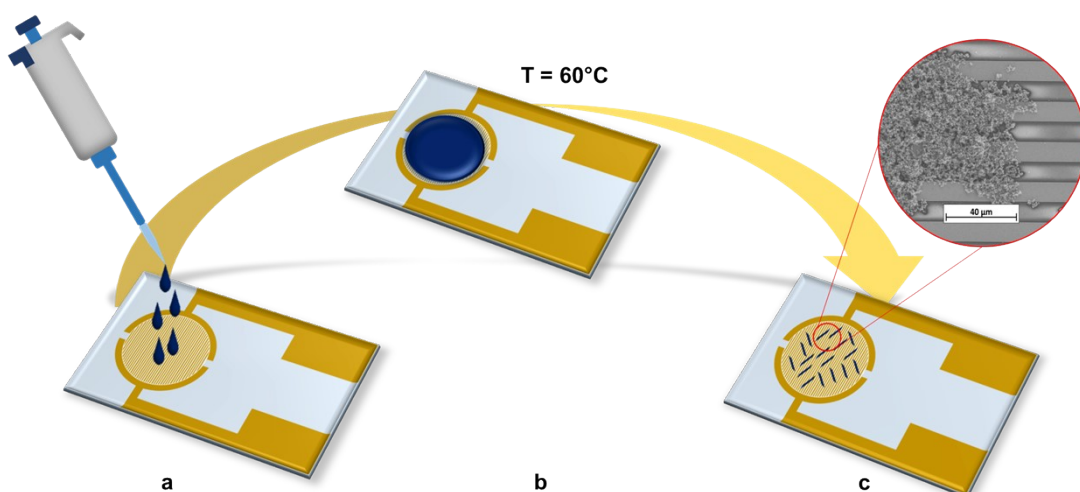


Fig. S1. Scheme of photodetector fabrication process: (a) drop-casting of Bi_2S_3 dispersion in ethanol onto ED-IDE1-Au chip, (b) solvent evaporation at 60°C , and (c) final chip-based photodetector with deposited particles. An inset in figure (c) shows SEM micrograph of the Bi_2S_3 ($\text{BS-PVA}_{\text{high}}$ sample) deposited on the ED-IDE1-Au chip.

Table S1. A comparison of the energy band gaps of BS, BS-PVA_{low}, and BS-PVA_{high} samples with literature data for Bi₂S₃ (used abbreviations: T – theoretical computations performed using first principle Density Functional Theory (DFT), E – experimental method of energy band gap determination based on UV-VIS spectroscopy).

Material	Method of material preparation	Energy band gap value, eV	Band gap type	Determination method	Ref.
Bi ₂ S ₃ film	atomic layer deposition	1.03	indirect	E	[1]
Bi ₂ S ₃	not applicable	1.32	indirect	T	[2]
Bi ₂ S ₃ film	physical vapor deposition	1.32 – 1.36		E	[3]
Bi ₂ S ₃ film	reactive evaporation	1.38	direct	E	[4]
Bi ₂ S ₃ nanoflowers	hydrothermal method	1.39	direct	E	[5]
Bi ₂ S ₃ film	electrochemical synthesis	1.4	direct	E	[6]
Bi ₂ S ₃ nanosheets	hydrothermal vulcanization	1.41	direct	E	[7]
Bi ₂ S ₃ nanocrystals	organometallic synthesis	1.443		E	[8]
Bi ₂ S ₃ nanowires	hydrothermal vulcanization	1.46	direct	E	[7]
Bi ₂ S ₃ nanoribbons	hydrothermal vulcanization	1.47	direct	E	[7]
Bi ₂ S ₃	not applicable	1.492	indirect	T	[9]
Bi ₂ S ₃ film	atomic layer deposition	1.56	direct	E	[1]
Bi ₂ S ₃ film	chemical bath deposition	1.56	direct	E	[10]
Bi ₂ S ₃ film	successive ionic layer adsorption and reaction	1.61	direct	E	[11]
Bi ₂ S ₃ film	pulse-plating method	1.68	direct	E	[12]
BS	microwave synthesis	1.34(2)	direct	E	this work
BS-PVA _{high}	PVA-assisted microwave synthesis	1.41(1)	direct	E	this work
BS-PVA _{low}	PVA-assisted microwave synthesis	1.43(3)	direct	E	this work

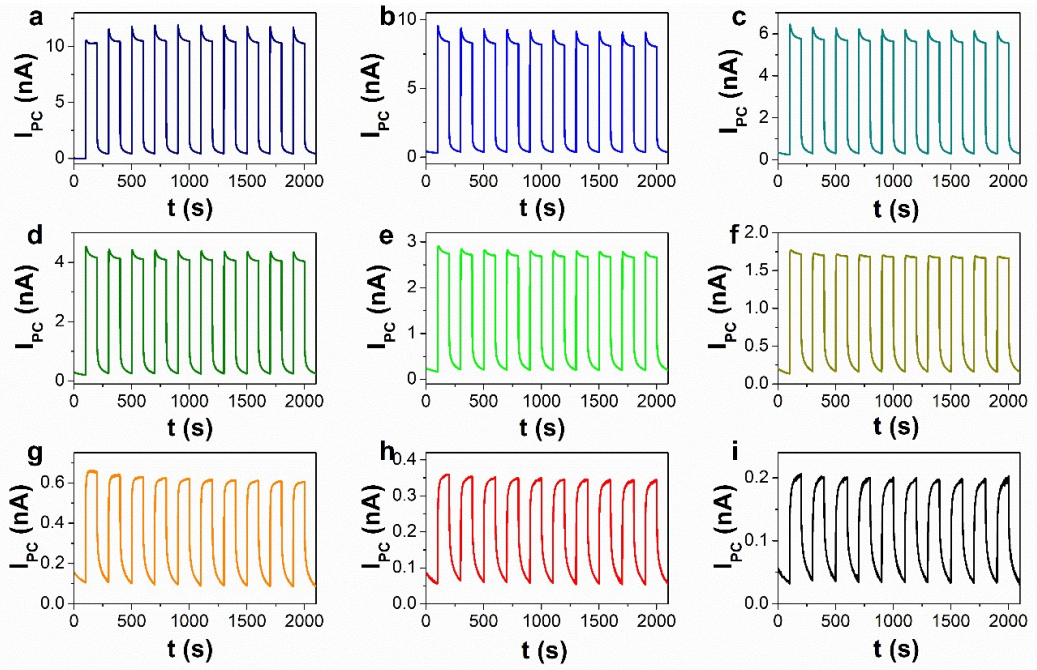


Fig. S2. The transient photocurrent responses of Bi_2S_3 nanosheets (BS-PVA_{high} sample) to switching ON and OFF green light illumination ($\lambda=517 \text{ nm}$) measured for different light intensities (a) $I_L=915 \mu\text{W}/\text{cm}^2$, (b) $I_L=619 \mu\text{W}/\text{cm}^2$, (c) $I_L=323 \mu\text{W}/\text{cm}^2$, (d) $I_L=183 \mu\text{W}/\text{cm}^2$, (e) $I_L=86 \mu\text{W}/\text{cm}^2$, (f) $I_L=36 \mu\text{W}/\text{cm}^2$, (g) $I_L=5.9 \mu\text{W}/\text{cm}^2$, (h) $I_L=2.3 \mu\text{W}/\text{cm}^2$, (i) $I_L=0.95 \mu\text{W}/\text{cm}^2$ ($U=1 \text{ V}$, $T=20^\circ\text{C}$, $RH=30\%$).

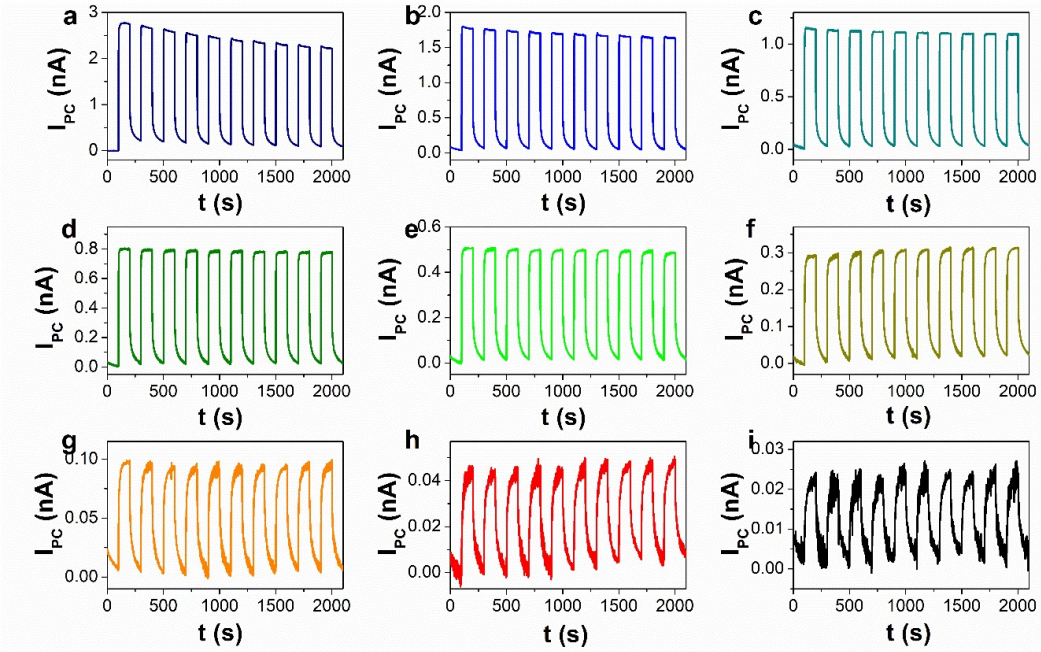


Fig. S3. The transient photocurrent responses of Bi_2S_3 nanosheets (BS-PVA_{high} sample) to switching ON and OFF red light illumination ($\lambda=628 \text{ nm}$) measured for different light intensities (a) $I_L=332 \mu\text{W}/\text{cm}^2$, (b) $I_L=202 \mu\text{W}/\text{cm}^2$, (c) $I_L=92 \mu\text{W}/\text{cm}^2$, (d) $I_L=48 \mu\text{W}/\text{cm}^2$, (e) $I_L=20 \mu\text{W}/\text{cm}^2$, (f) $I_L=7.7 \mu\text{W}/\text{cm}^2$, (g) $I_L=0.98 \mu\text{W}/\text{cm}^2$, (h) $I_L=0.34 \mu\text{W}/\text{cm}^2$, (i) $I_L=0.13 \mu\text{W}/\text{cm}^2$ ($U=1 \text{ V}$, $T=20^\circ\text{C}$, $RH=30\%$).

References

1. Mahuli N, Saha D, Sarkar SK. Atomic Layer Deposition of p-Type Bi₂S₃. *J Phys Chem C* [Internet]. 2017(e)ko apirlakaren 13a;121(14):8136–44. Available at: <https://doi.org/10.1021/acs.jpcc.6b12629>
2. Koc H, Ozisik H, Deligöz E, Mamedov AM, Ozbay E. Mechanical, electronic, and optical properties of Bi₂S₃ and Bi₂Se₃ compounds: first principle investigations. *J Mol Model* [Internet]. 2014(e)ko ;20(4):2180. Available at: <https://doi.org/10.1007/s00894-014-2180-1>
3. ten Haaf S, Sträter H, Brüggemann R, Bauer GH, Felser C, Jakob G. Physical vapor deposition of Bi₂S₃ as absorber material in thin film photovoltaics. *Thin Solid Films* [Internet]. 2013(e)ko ;535:394–7. Available at: <https://www.sciencedirect.com/science/article/pii/S0040609012015866>
4. Lukose J, Pradeep B. Electrical and optical properties of bismuth sulphide [Bi₂S₃] thin films prepared by reactive evaporation. *Solid State Commun* [Internet]. 1991(e)ko ;78(6):535–8. Available at: <https://www.sciencedirect.com/science/article/pii/0038109891903712>
5. Sharma S, Khare N. Sensitization of narrow band gap Bi₂S₃ hierarchical nanostructures with polyaniline for its enhanced visible-light photocatalytic performance. *Colloid Polym Sci* [Internet]. 2018(e)ko ;296(9):1479–89. Available at: <https://doi.org/10.1007/s00396-018-4362-3>
6. Grubač Z, Katić J, Metikoš-Huković M. Energy-Band Structure as Basis for Semiconductor n-Bi₂S₃/n-Bi₂O₃ Photocatalyst Design. *J Electrochem Soc* [Internet]. 2019(e)ko ;166(10):H433. Available at: <https://dx.doi.org/10.1149/2.0481910jes>
7. Liang YC, Li TH. Controllable morphology of Bi₂S₃ nanostructures formed via hydrothermal vulcanization of Bi₂O₃ thin-film layer and their photoelectrocatalytic performances. 2022(e)ko ;11(1):284–97. Available at: <https://doi.org/10.1515/ntrev-2022-0016>
8. Aresti M, Saba M, Piras R, Marongiu D, Mula G, Quochi F, et al. Colloidal Bi₂S₃ Nanocrystals: Quantum Size Effects and Midgap States. *Adv Funct Mater* [Internet]. 2014(e)ko ekainakaren 1a;24(22):3341–50. Available at: <https://doi.org/10.1002/adfm.201303879>
9. Ben Abdallah H, Ouerghui W. Spin-orbit coupling effect on electronic, linear and nonlinear optical properties of Bi₂S₃ and the ternary bismuth sulfide Bi₂S_{2.75}Se_{0.25}: Ab-initio calculations. *Opt Quantum Electron* [Internet]. 2021(e)ko ;54(1):20. Available at: <https://doi.org/10.1007/s11082-021-03411-y>
10. Moreno-García H, Messina S, Calixto-Rodriguez M, Martínez H. Physical properties of chemically deposited Bi₂S₃ thin films using two post-deposition treatments. *Appl Surf Sci* [Internet]. 2014(e)ko ;311:729–33. Available at: <https://www.sciencedirect.com/science/article/pii/S0169433214011878>
11. Suresh Kumar M, Madhusudanan SP, Mohanta K, Batabyal SK. Development and characterization of photodiode from p-Cu₂CdSnS₄/n-Bi₂S₃ heterojunction. *Mater Res Express* [Internet]. 2020(e)ko ;7(1):15909. Available at: <https://dx.doi.org/10.1088/2053-1591/ab65e1>
12. Ding F, Wang Q, Zhou S, Zhao G, Ye Y, Ghomashchi R. Synthesis of Bi₂S₃ thin films based on pulse-plating bismuth nanocrystallines and its photoelectrochemical properties. *R Soc Open Sci* [Internet]. 2020(e)ko abuztuakaren 12a;7(8):200479. Available at: <https://doi.org/10.1098/rsos.200479>